DALTON
FULL PAPER

Synthesis, spectroscopic and structural studies on rhodium-(I) and -(III) and iridium-(I) and -(III) selenoether and telluroether complexes involving organometallic co-ligands

William Levason, Simon D. Orchard, Gillian Reid and Joan M. Street

Department of Chemistry, University of Southampton, Highfield, Southampton, UK SO17 1BJ

Received 8th May 2000, Accepted 14th June 2000
Published on the Web 12th July 2000

Low and medium oxidation state organometallic complexes with triseleno- and telluro-ether ligands have been prepared. Reaction of $[M(COD)Cl]_2$ (M = Rh or Ir) with two molar equivalents of L^3 ($L^3 = MeC(CH_2ER)_3$, E = Se, R = Me; E = Te, R = Me or Ph) and two molar equivalents of NH_4PF_6 at room temperature in CH_2Cl_2 affords the species $[M(COD)(L^3)][PF_6]$. These complexes, which represent the first seleno- or telluro-ether complexes of Rh^I or Ir^I, have been characterised by analysis, IR and multinuclear NMR spectroscopy. The crystal structures of $[Rh(COD)\{MeC(CH_2SeMe)_3\}]PF_6$, $[Ir(COD)\{MeC(CH_2SeMe)_3\}]PF_6$, $[Rh(COD)\{MeC(CH_2TeMe)_3\}]PF_6$ and $[Ir(COD)\{MeC(CH_2TePh)_3\}]PF_6$ reveal distorted square pyramidal geometries. The rhodium(III) and iridium(III) complexes $[M(C_5Me_5)(L^3)][PF_6]_2$ have been prepared *via* the reaction of $[M(C_5Me_5)Cl_2]_2$ with 2 mol equivalents of L^3 and 4 of $TlPF_6$ in refluxing MeOH. Comparisons of the spectroscopic and crystallographic data for the metal(I) complexes reveal superior σ donation by the ligand $MeC(CH_2TeMe)_3$ compared with its selenoether analogue. In contrast, the medium oxidation state metal(III) complexes show enhanced donation by the selenoether ligand. The reaction of the COD complexes with H_2 is also described.

Introduction

Despite the fact that a range of ditelluroether ligands were reported over 10 years ago,[1] and thorough investigations into their co-ordination chemistry have been undertaken, there have been very few reports on the preparation and co-ordination chemistry of higher denticity telluroethers. Examples are limited to the tripodal $MeC(CH_2TeR)_3$ (R = Me or Ph),[1,2] spirocyclic $C(CH_2TePh)_4$ and one recently reported macrocyclic tritelluroether [12]aneTe$_3$ (1,5,9-tritelluracyclododecane).[3] We recently reported a detailed investigation into the species *fac*–$[MX(CO)_3(E\text{-}E)]$ (M = Mn or Re; X = Cl, Br or I; E-E = dithio-, diseleno- or ditelluro-ether) probing the relative donating abilities of Group 16 ligands and found that, in agreement with theoretical predictions by Schumann *et al.*,[4] telluroether ligands are significantly better σ donors to low valent metal centres than their lighter analogues.[5] The co-ordination chemistry of ditelluroether ligands with platinum group metals is well established,[6] and we have recently investigated the chemistry of the ligands $MeC(CH_2TeR)_3$ (R = Me or Ph) and, for comparison, $MeC(CH_2SeMe)_3$ with the platinum and Group 11 metals with the aim to form homoleptic species. As part of this work we reported the first homoleptic hexaseleno- and hexatelluro-ether complexes $[Ru\{MeC(CH_2EMe)_3\}_2][CF_3SO_3]_2$ (E = Se or Te)[7] and illustrated the versatility of these ligands in adopting various co-ordination modes as a consequence of metal ion requirements.[8]

The role of organometallic complexes with Group 16 ligands as catalysts is an area receiving increased attention, with the application of iridium complexes containing dithioether ligands in asymmetric hydrogenation being reported recently.[9] The reactions of monodentate heterocyclic organotellurium ligands with the pentamethylcyclopentadienylrhodium(III) dichloride dimer have also been reported as potential models for the initial steps in heterogeneously catalysed hydrodesulfurisation.[10,11] However the preparation of organometallic complexes with seleno- or telluro-ether ligands is generally limited to carbonyl containing species.

We report here the results of a study into the chemistry of the ligands, L^3, $MeC(CH_2TeR)_3$ (R = Me or Ph) and, for comparison, $MeC(CH_2SeMe)_3$ with the species $[M(COD)Cl]_2$ (COD = cycloocta-1,5-diene) and $[M(C_5Me_5)Cl_2]_2$ (M = Rh or Ir) to give the complexes $[M(COD)(L^3)][PF_6]$ and $[M(C_5Me_5)(L^3)][PF_6]_2$. These precursors were chosen since they provide convenient sources of the metal ions in oxidation state +1 and +3 respectively and thus the effect of metal oxidation state on these ligands may be established. The reaction chemistry of the COD complexes with H_2 is also discussed.

Results and discussion

Rhodium(I) and iridium(I) complexes

Reaction of $[M(COD)Cl]_2$ (M = Rh or Ir) with two molar equivalents of L^3 ($L^3 = MeC(CH_2ER)_3$, E = Se, R = Me; E = Te, R = Me or Ph) and two molar equivalents of NH_4PF_6 at room temperature in CH_2Cl_2 affords a yellow (selenoether) or orange-brown (telluroether) solution, from which the complexes $[M(COD)(L^3)][PF_6]$ can be isolated after removal of the precipitated NH_4Cl and addition of diethyl ether. IR spectroscopy on the products shows peaks consistent with free PF_6^- anion, co-ordinated L^3 and COD. The electrospray mass spectra confirmed the identity of the cation, showing clusters of peaks with the correct mass and isotopic distribution, corresponding to $[M(COD)(L^3)]^+$ in each case.

Co-ordination of selenium or tellurium to a metal centre in these systems leads to chirality at the chalcogen. The co-ordinated tripodal ligands may exist as two diastereoisomers, *syn* and *anti*, which may interconvert by pyramidal inversion at Se/Te, a process whose energy depends upon factors such as the metal present, the ligand structure, chelate ring size, and ligands *trans* to Se/Te.[12] For the d^8 complexes reported here, further complexity is anticipated from the structure of the complexes since the donor atoms on the tripod ligand are likely to be inequivalent. Considering this, the ^{1}H NMR spectra at 300 K for all six complexes were surprisingly simple, showing just one

Table 1 ^{77}Se-{^{1}H} and ^{125}Te-{^{1}H} NMR (CH_2Cl_2–$CDCl_3$, 300 K) data for the complexes [M(COD)(L^3)][PF_6]

Complex	$\delta(^{77}Se\text{-}\{^1H\})^a$	$\delta(^{125}Te\text{-}\{^1H\})^b$	$\Delta(^{77}Se)^c$	$\Delta(^{125}Te)^c$	$\delta(Te):\delta(Se)$
[Rh(COD){MeC($CH_2EMe)_3$}]$^+$	78.2	188.3 (79 Hz)	53.8	166.3	2.4
[Rh(COD){MeC($CH_2TePh)_3$}]$^+$	—	455.2	—	68	—
[Ir(COD){MeC($CH_2EMe)_3$}]$^+$	58.7	145.0	34.3	123.0	2.5
[Ir(COD){MeC($CH_2TePh)_3$}]$^+$	—	420.2	—	33	—

^{a} Relative to neat $SeMe_2$. ^{b} Relative to neat $TeMe_2$, $^1J_{Te\text{-}Rh}$ in parentheses. ^{c} $\delta_{complex} - \delta_{free\ ligand}$.

signal each for the EMe, CH_2 and MeC groups along with one signal each for the COD CH and CH_2 groups. This indicates that these complexes are probably fluxional in solution at room temperature, the dynamic processes involving the rotation of the ligands or the arms of the tripod rapidly flipping on and off the metal centre. Similar behaviour has been observed for the complexes $[M(L^3)_2]^{2+}$(M = Pd or Pt).[8] The ^{13}C-{^{1}H} NMR spectra were also recorded and showed one signal for each set of chemically different carbons in the COD or tripod ligand. This is consistent with ^{13}C-{^{1}H} and ^{1}H NMR data reported for the complex [Rh(COD)([9]aneS_3)][PF_6].[13]

Inspection of the ^{13}C-{^{1}H} and ^{1}H NMR data show that the COD CH group is more shielded in the complex [Rh(COD)-{MeC($CH_2TeMe)_3$}][PF_6] than in the other two rhodium complexes. This supports the superior σ donor properties of the ligand MeC($CH_2TeMe)_3$ to low valent metals, resulting in increased π back bonding from Rh to the π*(C=C) orbitals, compared to the methyl selenoether and phenyl telluroether tripod ligands. For the iridium complexes the δ(COD CH) are shifted to low frequency compared to those of the analogous rhodium complexes, indicating greater nuclear shielding from the heavier Ir. However the ^{13}C-{^{1}H} NMR spectra again show that the COD CH groups are more shielded in the methyl telluroether complex than the other two complexes, although the effect is less pronounced than that observed in the rhodium complexes.

In order to gain further information on the solution structure of these complexes ^{77}Se-{^{1}H}/^{125}Te-{^{1}H} NMR spectra were recorded. At room temperature the ^{77}Se-{^{1}H} and ^{125}Te-{^{1}H} NMR data (Table 1) show that for all six complexes only one resonance is observed, which confirms that the complexes are fluxional in solution and thus all three arms of the tripod appear equivalent. Rhodium coupling is only observed for the methyl telluroether complex with a doublet in the ^{125}Te-{^{1}H} NMR spectrum ($^1J_{Rh\text{-}Te}$ = 79 Hz), indicating that ligand dissociation does not occur during the fluxional process for this complex. This value is consistent with other ^{103}Rh–^{125}Te couplings reported.[14] When compared to the rhodium complexes, the ^{77}Se and ^{125}Te resonances are shifted to low frequency for the iridium complexes, again indicating greater nuclear shielding from the heavier Ir. In order to try to distinguish the different tellurium environments, the ^{125}Te-{^{1}H} NMR spectra were also recorded at 210 K for the samples [Rh(COD){MeC(CH_2-$TeR)_3$}][PF_6] (R = Me or Ph). However, no change from the room temperature spectrum was observed for the methyl telluroether complex, although for the phenyl ligand complex a broadening in the resonance was detected.

For many comparable organo-selenium and -tellurium compounds the ^{77}Se and ^{125}Te chemical shifts show very consistent trends and often the $\delta(Te):\delta(Se)$ ratio is 1.7–1.8 : 1.[15] Similar trends have been observed, by ourselves, for the diseleno- and ditelluro-ether complexes of Pd^{II} and Pt^{II}.[16] However, in our study of dithio-, diseleno- and ditelluro-ether complexes of manganese carbonyl halides we found that the ^{125}Te chemical shifts for the co-ordinated telluroethers were much more positive than expected, either by comparison with the ^{77}Se chemical shifts in the selenoether analogues or by comparison with the same ligands bound to medium oxidation state metal centres.[5] Indeed, the $\delta(Te):\delta(Se)$ ratio for these complexes ranged from 2.1 to 2.9 : 1. Thus we were interested to compare this ratio in the complexes of Rh^I and Ir^I reported here. Although the range of complexes is more limited the same trend is observed with $\delta(Te):\delta(Se)$ being 2.4 : 1 for the rhodium complexes and 2.5 : 1 for the iridium complexes, indicating superior σ donation by the telluroether ligand (Table 1).

Table 2 Selected bond lengths (Å) and angles (°) for [Rh(COD)-{Me($CH_2TeMe)_3$}]$^+$

Te(1)–Rh(1)	2.6226(8)	Te(2)–Rh(1)	2.5786(8)
Te(3)–Rh(1)	2.6924(7)	Rh(1)–C(9)	2.219(9)
Rh(1)–C(10)	2.178(8)	Rh(1)–C(15)	2.167(8)
Rh(1)–C(16)	2.135(8)		
Te(1)–Rh(1)–Te(3)	92.25(2)	Te(1)–Rh(1)–Te(2)	89.26(2)
Te(1)–Rh(1)–C(10)	101.0(2)	Te(1)–Rh(1)–C(9)	85.5(2)
Te(1)–Rh(1)–C(16)	164.5(2)	Te(1)–Rh(1)–C(15)	126.7(2)
Te(2)–Rh(1)–C(9)	152.8(3)	Te(2)–Rh(1)–Te(3)	87.11(2)
Te(2)–Rh(1)–C(15)	83.5(3)	Te(2)–Rh(1)–C(10)	167.9(2)
Te(3)–Rh(1)–C(9)	119.8(3)	Te(2)–Rh(1)–C(16)	90.7(2)
Te(3)–Rh(1)–C(15)	139.5(3)	Te(3)–Rh(1)–C(10)	86.1(3)
C(9)–Rh(1)–C(10)	36.5(4)	Te(3)–Rh(1)–C(16)	103.2(2)
C(9)–Rh(1)–C(16)	87.5(3)	C(9)–Rh(1)–C(15)	78.5(4)
C(10)–Rh(1)–C(16)	81.1(3)	C(10)–Rh(1)–C(15)	95.3(4)
C(15)–Rh(1)–C(16)	38.0(3)		

The preparation of the cyclooctene complexes [M($C_8H_{14})_2$-(L^3)]$^+$ (M = Rh or Ir) was also attempted *via* the reaction of [M($C_8H_{14})_2Cl]_2$ with two molar equivalents of L^3 and NH_4PF_6 in CH_2Cl_2. For rhodium a mixture of unidentified products was isolated that decomposed rapidly. The iridium complexes were slightly more stable, with the electrospray mass spectra showing a cluster of peaks corresponding to [Ir(C_8H_{14})L^3]$^+$, and IR spectroscopy displaying bands due to the tripodal ligand, cyclooctene and PF_6^-. However, the ^{1}H NMR spectra showed broad peaks indicating decomposition, and elemental analyses were consistently poor, and these studies were not pursued.

X-Ray crystallography

Owing to the fluxional nature of these complexes, limited structural information was obtained from NMR spectroscopy, therefore particular emphasis was placed on obtaining X-ray crystallographic data in order to ascertain the structural characteristics in the solid state. Since the metal centre in these complexes has a d^8 configuration, a square planar geometry might be expected with one of the tripod arms unco-ordinated, as observed for the complex [Pt{MeC($CH_2SeMe)_3$}$_2$]$^{2+}$.[8] However, for Rh^I and Ir^I although square planar complexes predominate, five-co-ordination also occurs, with the relative stability of five- and four-co-ordinate species depending upon the ligands involved.

Yellow or orange crystals of the complexes [Rh(COD)-{MeC($CH_2SeMe)_3$}][PF_6], [Rh(COD){MeC($CH_2TeMe)_3$}]-[PF_6], [Ir(COD){MeC($CH_2SeMe)_3$}][PF_6] and [Ir(COD){MeC-($CH_2TePh)_3$}][PF_6] were grown from the vapour diffusion of diethyl ether into solution of the complexes in MeCN (for the rhodium complexes) and Me_2CO (for the iridium complexes). The structure of [Rh(COD){MeC($CH_2TeMe)_3$}][PF_6] (Fig. 1, Table 2) shows the Rh^I co-ordinated to the COD and all three arms of the tripodal ligand. The methyl groups on the tripodal ligand adopt the *syn* arrangement. Hence the expected five-co-ordinate complex is obtained. Since both ligands in these

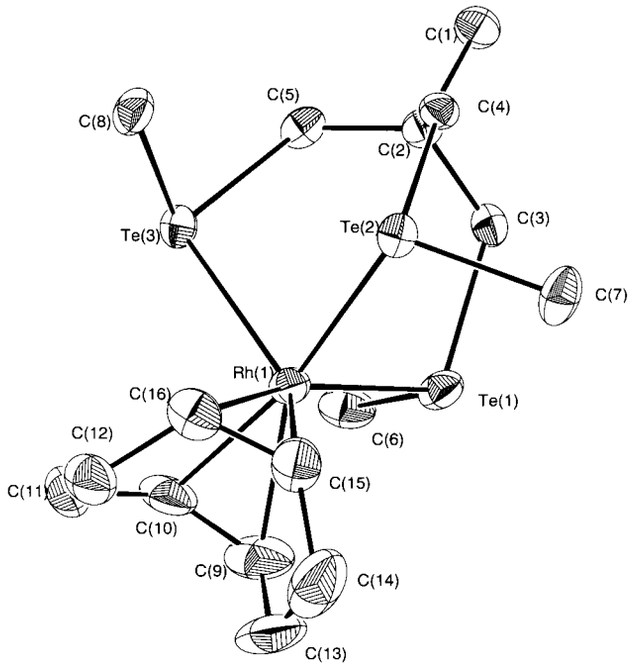

Fig. 1 View of the structure of $[Rh(COD)\{MeC(CH_2TeMe)_3\}]^+$ with the numbering scheme adopted. Ellipsoids in all cases are drawn at the 40% probability level.

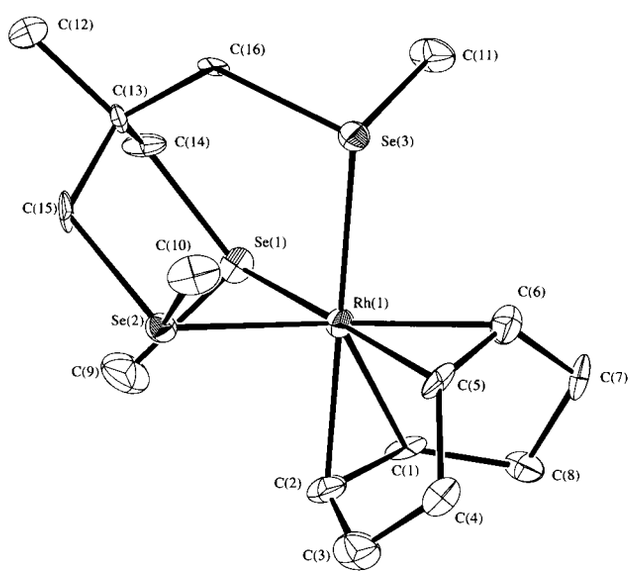

Fig. 2 View of the structure of $[Rh(COD)\{MeC(CH_2SeMe)_3\}]^+$. Details as in Fig. 1.

complexes are constrained, regular trigonal bipyramidal or square pyramidal geometries are not expected. Comparison of the bond lengths around the metal centre gives d(Rh–Te) = 2.6226(8), 2.5786(8), 2.6924(7) Å, thus one Rh–Te bond is notably longer than the other two. The Te–Rh–Te angles do not deviate significantly from 90°, with the Te–Rh–COD angles ranging from 83.5(3) to 167.9(2)°. Thus, the structure may best be described as square pyramidal with the longer Rh–Te bond axial and the shorter bonds being *trans* to the COD ligand.

The two selenoether complexes $[Rh(COD)\{MeC(CH_2SeMe)_3\}][PF_6]$ and $[Ir(COD)\{MeC(CH_2SeMe)_3\}][PF_6]$ (Figs. 2 and 3, Tables 3 and 4) are isostructural with d(Rh–Se) = (2.479(2), 2.483(2), 2.635(2) Å and d(Ir–Se) = 2.570(1), 2.481(1), 2.478(1) Å. The bond angles Se–M–Se are approximately 90°. The complex $[Ir(COD)\{MeC(CH_2TePh)_3\}][PF_6]$ (Fig. 4, Table 5) has d(Ir–Te) = 2.6033(8), 2.6062(7), 2.661(1) Å with again angles Te–Ir–Te not significantly deviating from 90°.

Table 3 Selected bond lengths (Å) and angles (°) for $[Rh(COD)\{MeC(CH_2SeMe)_3\}]^+$

Rh(1)–Se(1)	2.479(2)	Rh(1)–Se(2)	2.635(2)
Rh(1)–Se(3)	2.483(2)	Rh(1)–C(1)	2.18(1)
Rh(1)–C(2)	2.13(1)	Rh(1)–C(5)	2.13(1)
Rh(1)–C(6)	2.17(2)		
Se(1)–Rh(1)–Se(2)	89.64(7)	Se(1)–Rh(1)–Se(3)	90.55(7)
Se(1)–Rh(1)–C(1)	86.6(4)	Se(1)–Rh(1)–C(2)	96.1(5)
Se(1)–Rh(1)–C(5)	174.4(4)	Se(1)–Rh(1)–C(6)	138.3(4)
Se(2)–Rh(1)–Se(3)	85.29(6)	Se(2)–Rh(1)–C(1)	127.6(4)
Se(2)–Rh(1)–C(2)	90.3(5)	Se(2)–Rh(1)–C(5)	94.9(5)
Se(2)–Rh(1)–C(6)	129.8(4)	Se(3)–Rh(1)–C(1)	146.9(4)
Se(3)–Rh(1)–C(2)	172.0(5)	Se(3)–Rh(1)–C(5)	93.1(4)
Se(3)–Rh(1)–C(6)	81.3(4)	C(1)–Rh(1)–C(2)	38.6(6)
C(1)–Rh(1)–C(5)	88.0(6)	C(1)–Rh(1)–C(6)	79.1(6)
C(2)–Rh(1)–C(5)	80.6(6)	C(2)–Rh(1)–C(6)	96.6(6)

Table 4 Selected bond lengths (Å) and angles (°) for $[Ir(COD)\{MeC(CH_2SeMe)_3\}]^+$

Ir(1)–Se(1)	2.570(1)	Ir(1)–Se(2)	2.481(1)
Ir(1)–Se(3)	2.478(1)	Ir(1)–C(9)	2.17(1)
Ir(1)–C(10)	2.13(1)	Ir(1)–C(13)	2.15(1)
Ir(1)–C(14)	2.19(1)		
Se(1)–Ir(1)–Se(2)	86.44(4)	Se(1)–Ir(1)–Se(3)	90.21(4)
Se(1)–Ir(1)–C(9)	131.4(4)	Se(1)–Ir(1)–C(10)	95.7(3)
Se(1)–Ir(1)–C(13)	90.2(3)	Se(1)–Ir(1)–C(14)	126.5(3)
Se(2)–Ir(1)–Se(3)	90.79(4)	Se(2)–Ir(1)–C(9)	81.3(3)
Se(2)–Ir(1)–C(10)	92.8(3)	Se(2)–Ir(1)–C(13)	172.2(3)
Se(2)–Ir(1)–C(14)	146.9(3)	Se(3)–Ir(1)–C(9)	136.5(4)
Se(3)–Ir(1)–C(l0)	173.2(3)	Se(3)–Ir(1)–C(13)	96.3(3)
Se(3)–Ir(1)–C(14)	85.8(3)	C(9)–Ir(1)–C(10)	38.9(5)
C(9)–Ir(1)–C(13)	95.8(5)	C(9)–Ir(1)–C(14)	78.7(5)
C(10)–Ir(1)–C(13)	80.5(4)	C(10)–Ir(1)–C(14)	88.0(4)
C(13)–Ir(1)–C(14)	37.8(5)		

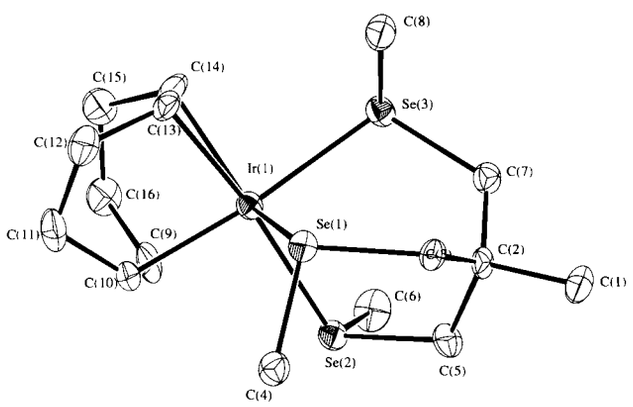

Fig. 3 View of the structure of $[Ir(COD)\{MeC(CH_2SeMe)_3\}]^+$. Details as in Fig. 1.

Hence these complexes show similar structural features to those of $[Rh(COD)\{MeC(CH_2TeMe)_3\}]^+$, *i.e.* a distorted square pyramidal geometry with the axial M–E bond significantly longer than the M–E bonds *trans* to COD. The R groups on the chalcogen adopt the *syn* arrangement. Interestingly, this is the only invertomer that we have observed in the crystal structures of these tripodal ligand complexes to date.

Since these complexes represent the first seleno- or telluroether rhodium(I) or iridium(I) complexes reported no direct comparisons from the literature are available. Structural data for series of complexes of Cu^I, Ag^I or Sn^{IV} have shown an increase in M–E of *ca.* 0.15 Å from E = Se to E = Te.[17] However, comparison of the structural data for the complexes $[Mn(CO)_3(L–L)X]$ (L–L = diseleno- or ditelluro-ether, X = Cl, Br or I) showed an increase in M–E of 0.13 Å.[5] For, these low valent complexes the increase in M–E is again smaller than

expected (0.1 Å) supporting spectroscopic data indicating greater σ donation of Te compared to that of Se.

Reactivity of COD complexes with H_2

The generation of transition metal hydride species is of interest due to their role in many catalytic hydrogenation processes. We were interested to establish whether these complexes would react with H_2 to form such species. In order to study this reaction, H_2 was bubbled through solutions of the complexes in CD_2Cl_2 at 0 °C and the ^{1}H NMR (360 MHz) spectra immediately recorded under an atmosphere of H_2 at 0 and −50 °C. Weak hydride resonances were observed only for the complex $[Ir(COD)\{MeC(CH_2SeMe)_3\}]^+$ at δ −13.01, −13.04 and −13.40 at 0 °C, which became more intense as the temperature was lowered to −50 °C. No change was observed in the spectra for the other complexes. These shifts are consistent with those obtained for iridium hydrides containing dithioether ligands.[9]

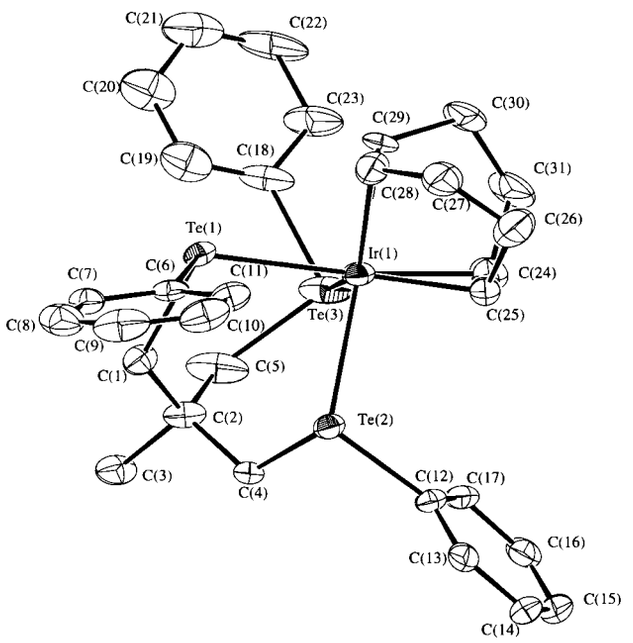

Fig. 4 View of the structure of $[Ir(COD)\{MeC(CH_2TePh)_3\}]^+$. Details as in Fig. 1.

Table 5 Selected bond lengths (Å) and angles (°) for $[Ir(COD)\{MeC(CH_2TePh)_3\}]^+$

Ir(1)–Te(1)	2.6033(8)	Ir(1)–Te(2)	2.6062(7)
Ir(1)–Te(3)	2.661(1)	Ir(1)–C(24)	2.19(1)
Ir(1)–C(25)	2.17(1)	Ir(1)–C(28)	2.17(1)
Ir(1)–C(29)	2.165(10)		
Te(1)–Ir(1)–Te(2)	84.70(2)	Te(1)–Ir(1)–Te(3)	87.39(3)
Te(1)–Ir(1)–C(24)	168.4(5)	Te(1)–Ir(1)–C(25)	152.5(5)
Te(1)–Ir(1)–C(28)	85.3(3)	Te(1)–Ir(1)–C(29)	92.3(3)
Te(2)–Ir(1)–Te(3)	95.93(3)	Te(2)–Ir(1)–C(24)	104.0(4)
Te(2)–Ir(1)–C(25)	87.8(3)	Te(2)–Ir(1)–C(28)	128.4(4)
Te(2)–Ir(1)–C(29)	166.7(4)	Te(3)–Ir(1)–C(24)	84.1(5)
Te(3)–Ir(1)–C(25)	119.8(5)	Te(3)–Ir(1)–C(28)	134.0(4)
Te(3)–Ir(1)–C(29)	96.9(4)	C(24)–Ir(1)–C(25)	37.7(6)
C(24)–Ir(1)–C(28)	94.9(5)	C(24)–Ir(1)–C(29)	80.9(4)
C(25)–Ir(1)–C(28)	78.7(4)	C(25)–Ir(1)–C(29)	89.0(4)
C(28)–Ir(1)–C(29)	38.3(5)		

Rhodium(III) and iridium(III) complexes

The extension of this chemistry to Rh^{III} and Ir^{III} was undertaken in order to study the properties of medium oxidation state organometallic complexes involving seleno- and telluroether ligands. Reaction of $[M(C_5Me_5)Cl_2]_2$ (M = Rh or Ir) with 2 mol equivalents of L^3 and 4 of $TlPF_6$ in refluxing MeOH afforded an orange solution and white precipitate of TlCl. After removal of the TlCl by filtration and concentration of the solutions *in vacuo*, the complexes $[Rh(C_5Me_5)(L^3)][PF_6]_2$ were isolated as orange solids upon addition of diethyl ether. The IR spectra showed the expected bands corresponding to the co-ordinated tripod ligand, C_5Me_5 and unco-ordinated PF_6^- anion. The electrospray mass spectra showed clusters of peaks with the correct isotopic distribution for $[M(C_5Me_5)(L^3)]^{2+}$. An X-ray data set was collected on a very small crystal of $[Ir(C_5Me_5)\{MeC(CH_2SeMe)_3\}][PF_6]_2$, but the data were too weak to afford a satisfactory refinement, although the expected pseudo-octahedral heavy atom framework was revealed. The ^{77}Se-{^{1}H} and ^{125}Te-{^{1}H} NMR spectra show one doublet for each of the three rhodium complexes (Table 6). Since inversion at an Rh^{III}–Se/TeR_2 unit is expected to be slow, this indicates the presence of just the *syn* invertomer.[8] In the iridium systems one resonance was present in $[Ir(C_5Me_5)\{MeC(CH_2TeMe)_3\}][PF_6]_2$ analogous to that of the rhodium complex and hence the *syn* isomer, whereas two resonances were observed for the complex with $MeC(CH_2SeMe)_3$ in the ratio 1 : 2 and hence this complex is the *anti* isomer. Three resonances were observed for the $MeC(CH_2TePh)_3$–Ir complex, indicating the presence of both *syn* and *anti* invertomers in solution. Comparing the shifts for L^3 with those for the COD complexes, a significant shift to high frequency is observed, as would be expected due to the higher oxidation state of the metal causing deshielding of the chalcogen. Upon changing from Rh to Ir, δ(Se) and δ(Te) are shifted to low frequency as observed for the complexes Rh^I and Ir^I. The ratio δ(Te) : δ(Se) for these +3 oxidation state complexes is expected to be nearer the norm of 1.7–1.8 : 1, since the contracted *n*d orbitals on the metal centre will result in poorer overlap between the tellurium atoms compared to that of the metal(I) species. This is indeed observed, with δ(Te) : δ(Se) = 2.1 : 1 for both the rhodium and iridium complexes with $MeC(CH_2EMe)_3$ (E = Se or Te). Thus, telluroether donation is less effective here compared to that in the COD complexes of Rh^I and Ir^I. For the rhodium complexes, coupling between rhodium and selenium or tellurium was observed in the form of doublets in the ^{125}Te-{^{1}H} or ^{77}Se-{^{1}H} NMR spectra. The value of $^1J_{Rh\text{-}Se}$ found for the selenoether complex (34 Hz) is slightly lower than those observed for other rhodium(III) selenoether complexes such as $[Rh\{MeC(CH_2SeMe)_3\}Cl_3]$ (*syn* 41 Hz, *anti* 39 Hz),[18] $[Rh\{MeC(CH_2SeMe)_3\}_2][PF_6]_3$ (43 Hz),[8] *trans*-$[RhCl_2([8]aneSe_2)_2][BF_4]$ ([8]$aneSe_2$ = 1,5-diselenacyclooctane, 42 Hz) and *cis*-$[RhCl_2([16]aneSe_4)][PF_6]$

Table 6 ^{13}C-{^{1}H} and ^{77}Se-{^{1}H}/^{125}Te-{^{1}H} NMR (MeCN–$CDCl_3$, 300 K) data for the complexes $[M(C_5Me_5)(L^3)][PF_6]_2$

Complex	$\delta(^{77}Se)^a$	$\delta(^{125}Te)^b$	$\delta(C_5Me_5)^c$
$[Rh(C_5Me_5)\{MeC(CH_2SeMe)_3\}]^{2+}$	126.6 (34)	—	100.2
$[Rh(C_5Me_5)\{MeC(CH_2TeMe)_3\}]^{2+}$	—	270.5 (91)	104.2
$[Rh(C_5Me_5)\{MeC(CH_2TePh)_3\}]^{2+}$	—	481.6 (91)	106.2
$[Ir(C_5Me_5)\{MeC(CH_2SeMe)_3\}]^{2+}$	98.1, 102.3	—	93.8
$[Ir(C_5Me_5)\{MeC(CH_2TeMe)_3\}]^{2+}$	—	214.5	98.5
$[Ir(C_5Me_5)\{MeC(CH_2TePh)_3\}]^{2+}$	—	394.2, 409.5, 449.1	94.4

[a] Relative to neat $SeMe_2$. $^1J_{Se\text{-}Rh}$ in parentheses. [b] Relative to neat $TeMe_2$, $^1J_{Te\text{-}Rh}$ in parentheses. [c] Relative to TMS.

([16]aneSe$_4$ = 1,5,9,13-tetraselenacyclohexadecane, 36, 37 Hz).[19] In contrast the $^1J_{Rh\text{-}Te}$ values observed for the telluroether complexes (Table 6) are larger than that found for the rhodium(I)–methyltelluroether COD complex and those reported for [Rh(L–L)$_2$Cl$_2$][PF$_6$] (L–L = MeTe(CH$_2$)$_3$TeMe, PhTe(CH$_2$)$_3$TePh or *o*-C$_6$H$_4$(TeMe)$_2$) where $^1J_{Rh\text{-}Te}$ ranged from 50 to 70 Hz.[14] For comparable complexes the ^1J(Te–X) : ^{1}J(Se–X) ratio is generally *ca.* 2–3 : 1.[15] This trend is observed for the MeC(CH$_2$EMe)$_3$ complexes with ^1J(Rh–Te)/^1J(Rh–Se) = 2.6.

The ^{13}C-{^{1}H} NMR spectra were recorded to examine changes at the C$_5$Me$_5$ group. Comparison of shifts for the complexes of Rh and Ir shows that upon changing the metal centre from Rh to Ir a shift to low frequency is again found. Interestingly, δ(*C*$_5$Me$_5$) is shifted to high frequency upon changing the donor from Se to Te. This trend is observed for both the rhodium and iridium complexes and indicates that the C$_5$Me$_5$ ligand is more shielded in the selenoether complex than in the telluroether complex. Hence, as the donor is changed from Se to Te, less electron density is transferred to the metal, resulting in decreased π acceptance by the C$_5$Me$_5$ group. This indicates that, for these medium oxidation state complexes, selenium is a stronger σ donor than tellurium, probably due to poor overlap between the large tellurium σ-donor orbital and the contracted metal orbitals.

Experimental

Infrared spectra were measured as CsI discs using a Perkin-Elmer 983 spectrometer over the range 200–4000 cm^{-1}, UV/vis spectra in solution using 1 cm path length quartz cells on a Perkin-Elmer Lambda19 spectrometer, mass spectra by positive electrospray (ES$^+$) using a VG Biotech Platform and ^{1}H NMR spectra, unless otherwise stated, using a Bruker AM300 spectrometer operating at 300 MHz, ^{13}C-{^{1}H} ^{77}Se-{^{1}H} and ^{125}Te-{^{1}H} NMR spectra on a Bruker AM360 spectrometer operating at 90.6, 68.7 and 113.6 MHz respectively and referenced to neat TMS, Me$_2$Se and Me$_2$Te (δ 0). The ^{1}H NMR spectra for the *in situ* hydride experiments were recorded on a Bruker AM360 spectrometer operating at 360 MHz. Microanalyses were performed by the microanalytical service of Strathclyde University. The complexes [Rh(COD)Cl]$_2$,[20] [Ir(COD)Cl]$_2$,[21] [Rh(C$_5$Me$_5$)Cl$_2$]$_2$ and [Ir(C$_5$Me$_5$)Cl$_2$]$_2$ were prepared by the literature procedures[22] as were the ligands MeC(CH$_2$SeMe)$_3$,[23] MeC(CH$_2$TeMe)$_3$,[1] and MeC(CH$_2$TePh)$_3$.[2] All preparations were conducted in dried solvents under a dinitrogen atmosphere.

Preparations

[Rh(COD){MeC(CH$_2$SeMe)$_3$}][PF$_6$]. [Rh(COD)Cl]$_2$ (55 mg, 1.1×10^{-4} mol) was added to MeC(CH$_2$SeMe)$_3$ (80 mg, 2.2×10^{-4} mol) and NH$_4$PF$_6$ (39 mg, 2.4×10^{-4} mol) in CH$_2$Cl$_2$ (30 cm^3) and the mixture stirred at room temperature for 1 hour. The precipitated NH$_4$Cl was removed by filtration, the solvent volume reduced to 2 cm^3 *in vacuo* and diethyl ether added (10 cm^3) to give an orange precipitate. Yield 105 mg, 68% (Found: C, 26.6; H, 3.7. Calc. for C$_{16}$H$_{30}$F$_6$PRhSe$_3$: C, 27.2; H, 4.2%). ^{1}H NMR (CD$_3$CN): δ 1.22 (s, 3 H, CCH$_3$), 2.23 (s, 9 H, SeCH$_3$), 2.40 (br, 8 H, COD CH$_2$), 2.68 (s, 6 H, SeCH$_2$) and 3.96 (br, 4 H, COD CH). ^{13}C-{^{1}H} NMR (CH$_2$Cl$_2$–CDCl$_3$): δ 13.5 (SeCH$_3$), 32.2 (C*C*H$_3$), 32.7 (COD CH$_2$), 35.7 (SeCH$_2$) and 80.8 (COD CH). ES$^+$ (MeCN): *m*/*z* = 561; calc. for [Rh(COD){MeC(CH$_2$^{80}SeMe)$_3$}]$^+$ 565. IR/cm^{-1}: 3017w, 2973w, 2940w, 2879w, 2830w, 1460w, 1420m, 1359m, 1267w, 1094m, 926m, 906w, 845s, 613w and 557m. UV/vis (MeCN)/cm^{-1} (ε_{mol}/dm^3 mol^{-1} cm^{-1}): 26 820 (920), 32 210 (3103) and 36 710 (4123).

[Rh(COD){MeC(CH$_2$TeMe)$_3$}][PF$_6$]. This was prepared similarly as a brown solid (67%) (Found: C, 22.0; H, 3.2. Calc. for C$_{16}$H$_{30}$F$_6$PRhTe$_3$: C, 22.5; H, 3.5%). ^{1}H NMR (CD$_3$CN): δ 1.52 (s, 3 H, CCH$_3$), 2.06 (s, 9 H, TeCH$_3$), 2.43 (br, 8 H, COD CH$_2$), 2.51 (s, 6 H, TeCH$_2$) and 3.82 (br, 4 H, COD CH). ^{13}C-{^{1}H} NMR (CH$_2$Cl$_2$–CDCl$_3$): δ −10.5 (TeCH$_3$), 14.4 (TeCH$_2$), 31.6 (C*C*H$_3$), 32.3 (COD CH$_2$) and 76.4 (COD CH). ES$^+$ (MeCN): *m*/*z* = 709; calc. for [Rh(COD){MeC(CH$_2$-^{130}TeMe)$_3$}]$^+$ 715. IR/cm^{-1}: 1359s, 1096s, 987m, 836s, 613w and 558m. UV/vis (MeCN)/cm^{-1} (ε_{mol}/dm^3 mol^{-1} cm^{-1}): 24 880 (6133) and 31 150 (9853).

[Rh(COD){MeC(CH$_2$TePh)$_3$}][PF$_6$]. This was prepared in a similar manner as an orange solid (69%) (Found: C, 34.6; H, 2.9. Calc. for C$_{31}$H$_{36}$F$_6$PRhTe$_3$·CH$_2$Cl$_2$: C, 34.2; H, 3.2%). ^{1}H NMR (CD$_3$CN): δ 1.58 (s, 3 H, CCH$_3$), 2.60 (s, 8 H, COD CH$_2$), 2.73 (s, 6 H, TeCH$_2$), 3.99 (s, 4 H, COD CH) and 7.4–7.7 (m, 15 H, TePh).^{13}C-{^{1}H} NMR (CH$_2$Cl$_2$–CDCl$_3$): δ 20.4 (TeCH$_2$), 32.0 (C*C*H$_3$), 32.6 (COD CH$_2$), 79.3 (COD CH), 111.9, 129.7, 130.0, 135.2 (TePh). ES$^+$ (MeCN): *m*/*z* = 895; calc. for [Rh(COD){MeC(CH$_2$^{130}TePh)$_3$}]$^+$ 901. IR/cm^{-1}: 3050w, 2951w, 2896w, 1571w, 1474m, 1433w, 1405w, 1359m, 1262w, 1235w, 1094m, 1016w, 997w, 840s, 740m, 693m, 613w, 558s and 454m. UV/vis (MeCN)/cm^{-1} (ε_{mol}/dm^3 mol^{-1} cm^{-1}): 22 520 (645), 31 250 (4950) and 38 760 (14 215).

[Ir(COD){MeC(CH$_2$SeMe)$_3$}][PF$_6$]. This was prepared similarly using [Ir(COD)Cl]$_2$ instead of [Rh(COD)Cl]$_2$ to give a yellow solid (66%) (Found: C, 23.9; H, 3.4. Calc. for C$_{16}$H$_{30}$F$_6$IrPSe$_3$: C, 24.1; H, 3.8%). ^{1}H NMR (CD$_3$CN): δ 1.21 (s, 3 H, CCH$_3$), 2.24 (br, 8 H, COD CH$_2$), 2.37 (s, 9 H, SeCH$_3$), 2.65 (s, 6 H, SeCH$_2$) and 3.96 (br, 4 H, COD CH). ^{13}C-{^{1}H} NMR (CH$_2$Cl$_2$–CDCl$_3$): δ 16.6 (SeCH$_3$), 32.8 (C*C*H$_3$), 33.7 (COD CH$_2$), 36.8 (SeCH$_2$) and 62.3 (COD CH). ES$^+$ (MeCN): *m*/*z* = 651; calc. for [^{193}Ir(COD){MeC(CH$_2$^{80}SeMe)$_3$}]$^+$ 655. IR/cm^{-1}: 2973w, 2918w, 2841w, 1416m, 1356s, 1095s, 991m, 930w, 905w, 846s, 613w and 557m. UV/vis (MeCN)/cm^{-1} (ε_{mol}/dm^3 mol^{-1} cm^{-1}): 22 075 (50), 25 000 (255), 27 100 (450) and 32 790 (305).

[Ir(COD){MeC(CH$_2$TeMe)$_3$}][PF$_6$]. This was prepared similarly as a brown solid (31%) (Found: C, 19.9; H, 2.5. Calc. for C$_{16}$H$_{30}$F$_6$IrPTe$_3$: C, 20.4; H, 3.2%). ^{1}H NMR (CD$_3$CN): δ 1.47 (s, 3 H, CCH$_3$), 2.11 (s, 9 H, TeCH$_3$), 2.35 (br, 8 H, COD CH$_2$), 2.57 (s, 6 H, TeCH$_2$) and 3.42 (br, 4 H, COD CH). ^{13}C-{^{1}H} NMR (CH$_2$Cl$_2$–CDCl$_3$): δ −8.3 (TeCH$_3$), 14.0 (TeCH$_2$), 34.1 (C*C*H$_3$), 36.3 (COD CH$_2$) and 61.8 (COD CH). ES$^+$ (MeCN): *m*/*z* = 799; calc. for [^{193}Ir(COD){MeC(CH$_2$^{130}TeMe)$_3$}]$^+$ 805. IR/cm^{-1}: 2962w, 1359s, 1261w, 1091s, 991m, 841s, 613w and 557m. UV/vis (MeCN)/cm^{-1} (ε_{mol}/dm^3 mol^{-1} cm^{-1}): 19 420 (130), 30 120 (2930) and 37 880 (9890).

[Ir(COD){MeC(CH$_2$TePh)$_3$}][PF$_6$]. This was prepared in a similar manner as an orange solid (64%) (Found: C, 32.5; H, 2.5. Calc. for C$_{31}$H$_{36}$F$_6$IrPTe$_3$: C, 33.0; H, 3.2%). ^{1}H NMR (CD$_3$CN): δ 1.43 (s, 3 H, CCH$_3$), 2.35 (s, 8 H, COD CH$_2$), 2.52 (s, 6 H, TeCH$_2$), 3.82 (s, 4 H, COD CH) and 7.4–7.7 (m, 15 H, TePh). ^{13}C-{^{1}H} NMR (CH$_2$Cl$_2$–CDCl$_3$): δ 20.3 (TeCH$_2$), 33.3 (CCH$_3$), 36.7 (COD CH$_2$), 64.3 (COD CH), 111.9, 131.1, 135.4 (TePh). ES$^+$ (MeCN): *m*/*z* = 985; calc. for [^{193}Ir(COD){MeC-(CH$_2$^{130}TePh)$_3$}]$^+$ 991. IR/cm^{-1}: 2995w, 2951w, 1571w, 1474w, 1434w, 1359s, 1236w, 1092s, 1016w, 997m, 842s, 741s, 693m, 613w, 558s and 434m. UV/vis (MeCN)/cm^{-1} (ε_{mol}/dm^3 mol^{-1} cm^{-1}): 27 780 (20 560) and 39 370 (16 890).

[Rh(C$_5$Me$_5$){MeC(CH$_2$SeMe)$_3$}][PF$_6$]$_2$. To a solution of MeC(CH$_2$SeMe)$_3$ (57 mg, 1.6×10^{-4} mol) in MeOH (40 cm^3) was added TlPF$_6$ (3.2×10^{-4} mol) and [Rh(C$_5$Me$_5$)Cl$_2$]$_2$ (50 mg, 8.1×10^{-5} mol). The reaction mixture was refluxed for 18 hours to give an orange solution and white precipitate of TlCl. After filtration and reduction of the solvent volume *in vacuo* to 2 cm^3, addition of diethyl ether (10 cm^3) produced a light orange solid, which was subsequently recrystallised from MeCN and diethyl

Table 7 Crystallographic data collection and refinement parameters

	[Rh(COD){MeC-$(CH_2SeMe)_3$}]PF_6	[Rh(COD){MeC-$(CH_2TeMe)_3$}]PF_6	[Ir(COD){MeC-$(CH_2SeMe)_3$}]PF_6	[Ir(COD){$MeC(CH_2TePh)_3$}]-PF_6·0.5Me_2CO
Formula	$C_{16}H_{30}F_6PRhSe_3$	$C_{16}H_{30}F_6PRhTe_3$	$C_{16}H_{30}F_6IrPSe_3$	$C_{32.5}H_{39}F_6IrO_{0.5}PTe_3$
M	707.16	853.08	796.48	1157.65
Space group	$P2_1/n$	$C2/c$	$P2_1/n$	$C2/c$
Crystal system	Monoclinic	Monoclinic	Monoclinic	Monoclinic
a/Å	12.857(3)	27.203(3)	12.889(4)	22.330(4)
b/Å	12.278(3)	14.998(4)	12.274(6)	14.57(2)
c/Å	14.514(3)	12.658(3)	14.492(3)	23.67(1)
β/°	105.40(2)	114.75(1)	105.28(2)	107.55(2)
V/Å^3	2209.0(7)	4689(1)	2211(7)	7342(10)
Z	4	8	4	8
μ(Mo-Kα)/cm^{-1}	58.38	45.02	111.15	60.81
Unique obs. Reflections	4098	4303	4102	6732
Obs. reflections with [$I_o > 2\sigma(I_o)$]	1792	2906	3014	5221
R	0.048	0.028	0.038	0.041
R_w	0.054	0.034	0.049	0.058

ether. Yield 60 mg, 84% (Found: C, 24.1; H, 2.6. Calc. for $C_{18}H_{33}F_{12}P_2RhSe_3$: C, 24.6; H, 3.8%). ^{1}H NMR ($(CD_3)_2CO$): δ 1.00 (s, 3 H, CCH_3), 1.43 (s, 15 H, C_5Me_5), 2.62 (s, 9 H, $SeCH_3$) and 2.90–3.40 (br, 6 H, $SeCH_2$). ^{13}C-{^{1}H} NMR (CH_3CN–$CDCl_3$): δ 8.1 (C_5Me_5), 14.4 ($SeCH_3$), 29.6 (CCH_3), 34.6 ($SeCH_2$), 40.4 (CCH_3) and 100.2 (C_5Me_5). ES$^+$ (MeCN): m/z = 295; calc. for $[Rh(C_5Me_5)\{MeC(CH_2{}^{80}SeMe)_3\}]^{2+}$ 296. IR/cm^{-1}: 2907w, 1361m, 1096m, 1023w, 987w, 838s and 559m.

[Rh(C_5Me_5){$MeC(CH_2TeMe)_3$}][PF_6]$_2$. This was prepared similarly as a brown solid (75%) (Found: C, 21.4; H, 2.6. Calc. for $C_{18}H_{33}F_{12}P_2RhTe_3$: C, 21.1; H, 3.2%). ^{1}H NMR ($(CD_3)_2CO$): δ 1.40 (s, 3 H, CCH_3), 1.75 (s, 15 H, C_5Me_5), 2.05 (s, 9 H, $TeCH_3$) and 2.45 (s, 6 H, $TeCH_2$). ^{13}C-{^{1}H} NMR (CH_3CN–$CDCl_3$): δ −6.4 ($TeCH_3$), 9.3 (C_5Me_5), 17.9 ($TeCH_2$), 32.9 (CCH_3), 38.9 (CCH_3) and 104.2 (C_5Me_5). ES$^+$ (MeCN): m/z = 368; calc. for $[Rh(C_5Me_5)\{MeC(CH_2{}^{130}TeMe)_3\}]^{2+}$ 371. IR/cm^{-1}: 1474w, 1359s, 1095m, 839s, 740w, 614w and 559m.

[Rh(C_5Me_5){$MeC(CH_2TePh)_3$}][PF_6]$_2$. This was prepared similarly as a light orange solid (70%) (Found: C, 32.5; H, 2.5. Calc. for $C_{33}H_{39}F_{12}P_2RhTe_3$: C, 32.7; H, 3.2%). ^{1}H NMR ($(CD_3)_2CO$): δ 1.30 (s, 3 H, CCH_3), 1.48 (s, 15 H, C_5Me_5), 3.10–3.30 (br, 6 H, $TeCH_2$) and 7.4–7.7 (m, 15 H, TePh). ^{13}C-{^{1}H} NMR (CH_3CN–$CDCl_3$): δ 10.4 (C_5Me_5), 26.1 (CCH_3), 33.4 ($TeCH_2$), 40.9 (CCH_3), 106.2 (C_5Me_5) and 130–138 (TePh). ES$^+$ (MeCN): m/z = 461; calc. for $[^{103}Rh(C_5Me_5)\{MeC(CH_2{}^{130}TePh)_3\}]^{2+}$ 464. IR/cm^{-1}: 1359s, 1096s, 997m, 839s, 732m, 690w, 674w and 558m.

[Ir(C_5Me_5){$MeC(CH_2SeMe)_3$}][PF_6]$_2$. This was prepared similarly using $[Ir(C_5Me_5)Cl_2]_2$ instead of $[Rh(C_5Me_5)Cl_2]_2$ to give a yellow solid (65%) (Found: C, 22.8; H, 3.4. Calc. for $C_{18}H_{33}F_{12}IrP_2Se_3$: C, 22.3; H, 3.4%). ^{1}H NMR ($(CD_3)_2CO$): δ 1.46 (s, 3 H, CCH_3), 1.81 (s, 15 H, C_5Me_5), 2.15 (s, 9 H, $SeCH_3$) and 2.66 (s, 6 H, $SeCH_2$). ^{13}C-{^{1}H} NMR (CH_3CN–$CDCl_3$): δ 7.9 (C_5Me_5), 13.4, 13.9 ($SeCH_3$), 31.3 (CCH_3), 35.8, 36.2, 36.4 ($SeCH_2$), 42.3 (CCH_3) and 93.8 (C_5Me_5). ES$^+$ (MeCN): m/z = 715; calc. for $[^{193}Ir(C_5Me_5)\{MeC(CH_2{}^{80}SeMe)_3\}^{35}Cl]^+$ 717. IR/cm^{-1}: 1461w, 1359m, 1096m, 985w, 837s and 558m.

[Ir(C_5Me_5){$MeC(CH_2TeMe)_3$}][PF_6]$_2$. This was prepared similarly as a brown solid (55%) (Found: C, 19.0; H, 2.5. Calc. for $C_{18}H_{33}F_{12}IrP_2Te_3$: C, 19.4; H, 3.0%). ^{1}H NMR ($(CD_3)_2CO$): δ 1.60 (s, 3 H, CCH_3), 2.16 (s, 15 H, C_5Me_5), 2.39 (s, 9 H, $TeCH_3$) and 3.0–3.5 (s, 6 H, $TeCH_2$). ^{13}C-{^{1}H} NMR (CH_3CN–$CDCl_3$): δ −5.6 ($TeCH_3$), 8.8 (C_5Me_5), 15.6 ($TeCH_2$), 33.9 (CCH_3), 38.9 (CCH_3) and 98.5 (C_5Me_5). ES$^+$ (MeCN): m/z = 861; calc. for $[^{193}Ir(C_5Me_5)\{MeC(CH_2{}^{130}TeMe)_3\}^{35}Cl]^+$ 867. IR/cm^{-1}: 2940w, 1359s, 1098s, 986m, 841s, 740w, 697w, 615w and 558m.

[Ir(C_5Me_5){$MeC(CH_2TePh)_3$}][PF_6]$_2$. This was prepared similarly as a light orange solid (60%) (Found: C, 30.3; H, 2.3. Calc. for $C_{33}H_{39}F_{12}IrP_2Te_3$: C, 30.5; H, 3.0%). ^{1}H NMR ($(CD_3)_2CO$): δ 1.26 (s, 3 H, CCH_3), 1.63 (s, 15 H, C_5Me_5), 2.26 (s, 6 H, $TeCH_2$) and 7.2–7.8 (m, 15 H, TePh). ^{13}C-{^{1}H} NMR (CH_3CN–$CDCl_3$): δ 8.2 (C_5Me_5), 25.2 ($TeCH_2$), 29.9 (CCH_3), 40.6 (CCH_3), 94.4 (C_5Me_5) and 127–138 (TePh). ES$^+$ (MeCN): m/z = 1047; calc. for $[^{193}Ir(C_5Me_5)\{MeC(CH_2{}^{130}TePh)_3\}^{35}Cl]^+$ 1053. IR/cm^{-1}: 3061w, 1572w, 1475m, 1435m, 1360s, 1095s, 998m, 839s, 737m, 692m, 558m and 454w.

X-Ray crystallography

Details of the crystallographic data collection and refinement parameters are given in Table 7. Data collection used a Rigaku AFC7S four-circle diffractometer operating at 150 K, and graphite-monochromated Mo-K_α X-radiation (λ = 0.71073 Å). The data were corrected for absorption using ψ-scans (except for $[Rh(COD)\{MeC(CH_2SeMe)_3\}]PF_6$ for which ψ-scans did not provide a satisfactory correction, hence with the model at isotropic convergence the data were corrected for absorption using DIFABS).[24] The structures were solved by heavy atom Patterson methods[25] and developed by iterative cycles of full-matrix least-squares refinement and Fourier difference syntheses.[26] All non-H-atoms were refined anisotropically and H atoms were placed in fixed, calculated positions.

CCDC reference number 186/2029.

See http://www.rsc.org/suppdata/dt/b0/b003654o/ for crystallographic files in .cif format.

Acknowledgements

We thank the EPSRC for support and Johnson-Matthey plc for generous loans of platinum metal salts.

References

1 E. G. Hope, T. Kemmitt and W. Levason, *Inorg. Chem.*, 1988, **7**, 78.
2 J. C. Connolly, A. R. J. Genge, W. Levason, S. D. Orchard, S. J. A. Pope and G. Reid, *J. Chem. Soc., Dalton Trans.*, 1999, 2343.
3 Y. Takaguchi, E. Horn and N. Furukawa, *Organometallics*, 1996, **15**, 5112.
4 H. Schumann, A. A. Arif, A. L. Rheingold, C. Janiak, R. Hoffmann and N. Kuhn, *Inorg. Chem.*, 1991, **30**, 1618.
5 W. Levason, S. D. Orchard and G. Reid, *Organometallics*, 1999, **18**, 1275.
6 E. G. Hope and W. Levason, *Coord. Chem. Rev.*, 1993, **122**, 109.
7 W. Levason, S. D. Orchard and G. Reid, *Chem. Commun.*, 1999, 1071.

8 W. Levason, S. D. Orchard and G. Reid, *Inorg. Chem.*, in the press.
9 O. Pamies, M. Dieguez, G. Net, A. Ruiz and C. Claver, *J. Chem. Soc.*, *Dalton Trans.*, 1999, 3439.
10 K. Baydal, W. R. McWhinnie, H. L. Chen and T. A. Hamor, *J. Chem. Soc.*, *Dalton Trans.*, 1997, 1579.
11 K. Baydal, W. R. McWhinnie, J. Homer and M. C. Perry, *J. Organomet. Chem.*, 1998, **555**, 279.
12 E. W. Abel, K. G. Orrell, S. P. Scanlan, D. Stevenson, T. Kemmitt and W. Levason, *J. Chem. Soc.*, *Dalton Trans.*, 1991, 591.
13 A. J. Blake, R. O. Gould, M. Halcrow and M. Schroeder, *J. Chem. Soc.*, *Dalton Trans.*, 1994, 2197.
14 W. Levason, S. D. Orchard, G. Reid and V.-A. Tolhurst, *J. Chem. Soc.*, *Dalton Trans.*, 1999, 2071.
15 N. P. Luthra and J. D. Odom, in *The Chemistry of Organic Selenium and Tellurium Compounds*, eds. S. Patai and Z. Rappoport, Wiley, New York, 1986, vol. 1, Ch. 6.
16 T. Kemmitt, W. Levason and M. Webster, *Inorg. Chem.*, 1989, **28**, 692; T. Kemmmit and W. Levason, *Inorg. Chem.*, 1990, **29**, 731.
17 A. R. J. Genge, W. Levason and G. Reid, *J. Chem. Soc.*, *Dalton Trans.*, 1997, 4549.
18 E. G. Hope, W. Levason, G. L. Marshall and S. G. Murray, *J. Chem. Soc.*, *Dalton Trans.*, 1985, 2185.
19 W. Levason, J. J. Quirk and G. Reid, *J. Chem. Soc.*, *Dalton Trans.*, 1996, 3713.
20 G. Giodano and R. H. Crabtree, *Inorg. Synth.*, 1979, **19**, 218.
21 J. L. Herde, J. C. Lambert and C. V. Senoff, *Inorg. Synth.*, 1974, **15**, 18.
22 J. W. Kang, K. Moseley and P. M. Maitlis, *J. Am. Chem. Soc.*, 1969, **91**, 5970.
23 D. J. Gulliver, E. G. Hope, W. Levason, G. L. Marshall, S. G. Murray and D. M. Potter, *J. Chem. Soc.*, *Perkin Trans. 2*, 1984, 429.
24 N. Walker and D. Stuart, *Acta Crystallogr.*, *Sect. A*, 1983, **39**, 158.
25 Patty, The DIRDIF program System, P. T. Beurskens, G. Admiraal, G. Beurskens, W. P. Bosman, S. Garcia-Granda, R. O. Gould, J. M. M. Smits and C. Smykalla, Technical Report of the Crystallography Laboratory, University of Nijmegen, 1992.
26 TEXSAN, Crystal Structure Analysis Package, Molecular Structure Corporation, Houston, TX, 1995.